Tests of two forms of Stokes's integral using a synthetic gravity field based on spherical harmonics

Will E Featherstone

Abstract

Two gravimetric models of the geoid over Western Australia have been constructed using modified forms of Stokes's formula. The input data are synthetic gravity anomalies which have been generated by an artificial extension of the EGM96 global geopotential model to spherical harmonic degree and order 2700. This provides self-consistent sets of gravity anomalies and geoid heights, which are used as control on the effectiveness of a deterministically modified Stokes's kernel in relation to the common remove-restore technique with the spherical Stokes's kernel. The improved fit of the geoid model that uses a modification to allow for the neglect of the truncation error term and adapt its filtering properties indicates that the widely used remove-compute-restore approach is less appropriate for gravimetric geoid computation in the high-frequency band over Western Australia.

1 Introduction

In 1849, G. G. Stokes published a solution to the geodetic boundary value problem, which requires a global integration of gravity anomalies over the whole Earth to compute the separation (N) between the geoid and reference ellipsoid (Stokes, 1849). However, the incomplete global coverage and availability of accurate gravity measurements has precluded an exact determination of the geoid using Stokes's formula. Instead, an approximate solution is used in practice, where only gravity data in and close to the computation area are used. This approach is also attractive due to the increase in computational efficiency that is offered by working with a smaller integration area.

In 1958, M. S. Molodensky (cited in Molodensky *et al.*, 1962) proposed a modification to Stokes's formula to reduce the truncation error that results when gravity data are used over a limited area. However, Molodensky's modification did not receive a great deal of attention in practical geoid computations at that time because of the contemporaneous availability of low-frequency global gravity field information, derived from the analysis of the artificial Earth satellite orbits. These global geopotential models, expressed in terms of fully normalised spherical harmonics, are now routinely used in conjunction with terrestrial gravity data via a truncated form of Stokes's integral (eg. Vincent and Marsh, 1973; Sideris and She, 1995).

Assuming that the global geopotential model is a perfect fit to the low-degree terrestrial gravity field, this combined approach reduces the magnitude of the truncation error. This is because its Fourier series expansion begins at a higher degree, where the truncation coefficients are smaller in magnitude and the geopotential coefficients are expected to converge (cf. Grafarend and Engels, 1994). Another advantage of this combined solution is that it reduces the impact of the spherical approximation inherent to the derivation of Stokes's integral (eg. Heiskanen and Moritz, 1967); the reason being that most of the geoid's power is contained in the low-frequency band.

A formal description of the combination of a global geopotential model with terrestrial gravity data has been proposed by Vaníček and Sjöberg (1991), which they refer to as the generalised Stokes scheme for geoid computation. Importantly, this satisfies a solution to the geodetic boundary value problem when formulated for a higher than second-degree reference model (Martinec and Vaníček, 1997). In this generalised scheme, the low-frequency geoid undulations, computed from a global geopotential model (N_M), are extended into the high frequencies by a global integration of complementary high-frequency terrestrial gravity anomalies (Δg^M). This is written as

$$N = N_M + \kappa \int_0^{2\pi} \int_0^{\pi} S^M(\cos\psi)\ \Delta g^M\ \sin\psi\ d\psi\ d\alpha \tag{1}$$

where $\kappa = R/4\pi\gamma$, R is the spherical Earth radius, γ is normal gravity evaluated on the surface of the reference ellipsoid as required by Bruns's formula (eg. Heiskanen and Moritz, 1967), ψ and α are the coordinates of spherical distance and azimuth angle about the computation point, respectively, and $S^M(\cos\psi)$ is the spheroidal form of Stokes's kernel, which is implicit to the generalised scheme, and has the series expansion

$$S^M(\cos\psi) = \sum_{n=M+1}^{\infty} \frac{2n+1}{n-1}\ P_n(\cos\psi) \tag{2}$$

where $P_n(\cos\psi)$ is the n-th degree Legendre polynomial.

In Eq. (1), the low-frequency component of the geoid undulation (N^M) can be computed from the spherical harmonic coefficients that represent the global geopotential model according to

$$N_M = \frac{GM}{r\gamma} \sum_{n=2}^{M} \left(\frac{a}{r}\right)^n \sum_{m=0}^{n} (\delta\overline{C}_{nm}\cos m\lambda + \overline{S}_{nm}\sin m\lambda)\overline{P}_{nm}(\cos\theta) \tag{3}$$

The corresponding high-frequency gravity anomalies (Δg^M) are evaluated by subtracting the same spherical harmonic degrees of the same global geopotential model from the terrestrial gravity anomalies (Δg) according to

$$\Delta g^M = \Delta g - \frac{GM}{r^2} \sum_{n=2}^{M} \left(\frac{a}{r}\right)^n (n-1) \sum_{m=0}^{n} (\delta\overline{C}_{nm}\cos m\lambda + \overline{S}_{nm}\sin m\lambda)\overline{P}_{nm}(\cos\theta) \tag{4}$$

In Eqs. (3) and (4), GM is the product of the Newtonian gravitational constant and mass of the solid Earth, oceans and atmosphere, a is the equatorial radius of the geocentric reference ellipsoid, (r, θ, λ) are the geocentric polar coordinates of each computation point, $\delta\overline{C}_{nm}$ and $\overline{S}_{nm}$ are the fully normalised geopotential coefficients of degree n and order m, which have been reduced by the even zonal harmonics of the reference ellipsoid, and $\overline{P}_{nm}(\cos\theta)$ are the fully normalised associated Legendre functions. It is assumed that the zero and first degree harmonic terms are inadmissible (eg. Heiskanen and Moritz, 1967).

The degree of spheroid (M) used for the generalised Stokes scheme can be chosen as the maximum degree of global geopotential model available, which is usually $M_{max} = 360$. However, there are more important considerations than simply taking the maximum degree of expansion available (eg. Featherstone, 1992). Firstly, the $M_{max} = 360$ models are constructed from both satellite-derived and terrestrial gravity data. Therefore, in many regional geoid computations, the same terrestrial gravity data are used twice in Eq. (1). Clearly, this introduces the correlation of errors between these data, which are rarely accounted for nor even acknowledged by most authors.

Another consideration is the leakage of low-frequency errors from the terrestrial gravity data into the combined solution for the geoid, much of which can be filtered out by the spheroidal kernel in Eq. (2) (Vaníček and Featherstone, 1998). This is considered to be a desirable scenario, because the low-frequency geopotential coefficients are currently the best source of this information, whereas terrestrial gravity anomalies are subject to low-frequency errors. Therefore, choosing the degree of spheroid at, say, $M = 20$ (Vaníček and Kleusberg, 1987), which is probably the limit of the reliable resolution of the satellite-derived geopotential coefficients (notwithstanding resonant terms), avoids the correlations and reduces the leakage of terrestrial gravity anomaly errors.

2 Reduction of the Approximation Error

When high-frequency terrestrial gravity anomalies are used over a limited area, the generalised Stokes scheme becomes subject to a truncation error. Accordingly, there is an adjustment of Eq. (1) that involves limiting the integration domain to a spherical cap, bound by the spherical distance ψ_0 ($0 < \psi_0 < \pi$), which yields the approximation

$$\hat{N} \simeq N_M + \kappa \int_0^{2\pi} \int_0^{\psi_0} S^M(\cos\psi)\, \Delta g^M \; \sin\psi \, d\psi \, d\alpha \tag{5}$$

with a corresponding truncation error of

$$\delta N = \kappa \int_0^{2\pi} \int_{\psi_0}^{\pi} S^M(\cos\psi)\, \Delta g^M \; \sin\psi \, d\psi \, d\alpha \tag{6}$$

such that $N = \hat{N} + \delta N$. This truncation error can be expressed as a series expansion (eg. Vaníček and Featherstone, 1998) by

$$\delta N = 2\pi\kappa \sum_{n=M+1}^{\infty} Q_n^M(\psi_o)\, \Delta g_n \tag{7}$$

where the truncation coefficients

$$Q_n^M(\psi_o) = \int_{\psi_o}^{\pi} S^M(\cos\psi)\, P_n(\cos\psi)\, \sin\psi \, d\psi \tag{8}$$

can be evaluated using the algorithms of Paul (1973), and the n-th degree surface spherical harmonic of the gravity anomaly can be evaluated from the global geopotential model

$$\Delta g_n = \frac{GM}{r^2} \left(\frac{a}{r}\right)^n (n-1) \sum_{m=0}^{n} (\delta\overline{C}_{nm} \cos m\lambda + \overline{S}_{nm} \sin m\lambda) \overline{P}_{nm}(\cos\theta) \tag{9}$$

Therefore, the truncation error terms can be computed in the region $M \leq n \leq M_{max}$. If this is done, the truncation error then reduces to

$$\delta N = 2\pi\kappa \sum_{n=M_{max}+1}^{\infty} Q_n^M(\psi_o)\, \Delta g_n \tag{10}$$

However, if $\Delta g^M \neq 0$ ($2 \leq n \leq M$), the start of the series expansions in Eqs. (7) and (10) no longer hold, then there is a leakage of any low-frequency errors in the gravity data into the low-frequency geoid solution (when the integration is performed over a limited area; Vaníček and Featherstone, 1998). This is a direct consequence of the approximation of the generalised Stokes integral (Eq. 5), or any other gravity field convolution integral. Since Δg_n only depend on the physical properties of the Earth, it remains necessary to seek a modification of Stokes's integral that reduces the magnitude of the truncation error.

However, the common remove-compute-restore technique for the combined solution for the geoid (eg. Torge, 1991) makes no attempt to modify the integration kernel and thus reduce the truncation error or adapt its filtering properties. Instead, this scheme uses the spherical kernel as originally introduced by Stokes, which is

$$S(\cos\psi) = \sum_{n=2}^{\infty} \frac{2n+1}{n-1}\, P_n(\cos\psi) \tag{11}$$

Moreover, the remove-compute-restore approach generally uses the maximum degree (usually $M_{max} = 360$) of a global geopotential model to compute the residual gravity anomalies (Eq. 4). Accordingly, there is a disparity between the degree of the geopotential model and Stokes's kernel. The combined solution for the geoid in the remove-compute-restore scheme is thus written as

$$\hat{N}_1 \simeq N_{M_{max}} + \kappa \int_0^{2\pi} \int_0^{\psi_0} S(\cos\psi)\ \Delta g^{M_{max}}\ \sin\psi\ d\psi\ d\alpha \tag{12}$$

where the terms $N_{M_{max}}$ and $\Delta g^{M_{max}}$ are computed from the maximum available degree and order of a global geopotential model. In this combined solution for the geoid, little attempt has been made to reduce the truncation error or adapt the filtering properties of the spherical Stokes's kernel (Eq. 11). Admittedly, the truncation error has been reduced a great deal in the region ($2 \le n \le M_{max}$), if and only if the global geopotential model is a good fit to the terrestrial gravity anomalies over the area of interest. Conversely, this is at the expense of allowing any errors in the terrestrial gravity anomalies to propagate, virtually unattenuated, into the combined solution (Vaníček and Featherstone, 1998).

Accordingly, it remains preferable to apply a modification to the truncated form of the generalised Stokes integral (Eq. 5) or the truncated form of the spherical Stokes integral in the remove-compute-restore scheme (Eq. 12) to further reduce the errors associated with these approximations. Since Molodensky's pioneering work, several other authors have proposed modifications to Stokes's (1849) integral. These have been based on different criteria and can be broadly classified as deterministic modifications (eg. Molodensky *et al.* 1962; Wong and Gore 1969; Meissl 1971; Heck and Grüninger 1987; Vaníček and Kleusberg 1987; Vaníček and Sjöberg 1991; Featherstone *et al.* 1998) and stochastic modifications (eg. Wenzel 1982; Sjöberg 1991; Vaníček and Sjöberg 1991). The stochastic modifications, whilst offering an optimal combination (in a least-squares sense) of the data types together with a minimisation of the truncation error, require reliable error estimates of the input data. However, the error characteristics of the terrestrial gravity data are generally unknown, which renders the stochastic modifications of limited practical use. Therefore, the deterministic kernel modifications will have to be relied upon in the interim.

The deterministic kernel modifications can be further divided into two categories: modifications that reduce the truncation error according to some prescribed norm, and modifications that improve the rate of convergence of the series expansion of the truncation error. The modification scheme proposed by Featherstone *et al.* (1998) uses a combination of these, where the rate of convergence of the series expansion of an already-reduced truncation error is accelerated through a combination of the approaches proposed by Vaníček and Kleusberg (1987) and Meissl (1971). Essentially, this modification sets the Vaníček and Kleusberg (1987) kernel to zero at the truncation radius (ψ_0). Alternatively, the truncation radius can be chosen such that it coincides with a zero point of the Vaníček and Kleusberg (1987) kernel. This kernel modification can be written as

$$S_L^M(\cos\psi) = S^M(\cos\psi) - S^M(\cos\psi_0) - \sum_{k=2}^{L} \frac{2k+1}{2}\, t_k(\psi_0)\, [P_k(\cos\psi) - P_k(\cos\psi_0)] \tag{13}$$

where the modification coefficients $t_k(\psi_0)$ are computed from the solution of the following linear system of $L-1$ equations

$$\sum_{k=2}^{L} \frac{2k+1}{2}\, t_k(\psi_0)\, e_{nk}(\psi_0) = Q_n^M(\psi_0) \tag{14}$$

with

$$e_{nk}(\psi_0) = \int_{\psi_0}^{\pi} P_n(\cos\psi)\, P_k(\cos\psi) \sin\psi\, d\psi \tag{15}$$

which can be evaluated using the recursive algorithms of Paul (1973). The degree of this kernel modification (L) can be chosen to be greater than, equal to or less than the degree of the geopotential model (M) in the generalised Stokes formula (Eq. 5). However, if $L > M$, additional terms arise that account for this disparate combination and should be computed or their omission acknowledged.

The combined solution for the geoid considered in this study attempts to reach a compromise of the above two schemes, based on considerations of the data availability, their expected reliability and a reduction of the truncation error through the above deterministic modification of the generalised Stokes kernel. This compromise approach was used to compute the recent Australian gravimetric geoid model, AUSGeoid98 (Johnston and Featherstone, 1998). Mathematically, this is formalised as

$$\hat{N}_2 \simeq N_{M_{max}} + \kappa \int_0^{2\pi} \int_0^{\psi_0} S_L^M(\cos\psi)\, \Delta g^{M_{max}}\ \sin\psi\, d\psi\, d\alpha \tag{16}$$

where all terms have been defined earlier.

This utilises the maximum available expansion of the global geopotential model in conjunction with a low-degree deterministic kernel modification. This approach aims at reducing the truncation error so that it can be ignored, whilst relying more on the low-degree satellite solution by filtering a proportion of the low-frequency errors from the terrestrial gravity data. Empirical studies by Featherstone (1992) indicate that the modified kernels become numerically unstable for large L and small ψ_0, which enforces a low degree of kernel modification when a small integration radius is used. For simplicity, the degree of kernel modification is chosen equal to the degree of spheroid used in the generalised scheme (ie. $L = M = 20$). The integration radius was chosen to be $\psi_0 = 1°$, since this value was empirically selected for AUSGeoid98 (Johnston and Featherstone, 1998).

It is argued that this offers a geoid solution that is superior to the current remove-compute-restore approach because of its further reduction of the truncation error and adaption of the filtering properties of the kernel. However, it is also important to acknowledge the deficiencies of this attempted compromise, which are the reliance on the high-frequencies in the global geopotential model (which can contain 80% noise; eg. Lemoine *et al.*, 1998) and the correlations between the terrestrial gravity anomalies in the region $20 \leq M \leq 360$.

3 Tests with a synthetic gravity field in Western Australia

In order to compare the validity of the compromise in Eq. (16) and the remove-compute-restore technique (Eq. 12), a synthetic gravity field has been used. The expectation is that by using an error-free, self-consistent set of geoid heights and gravity anomalies, the effectiveness of each combined solution for the geoid can be determined. The approach is as follows: the synthetic gravity anomalies are reduced by the complete expansion of the global geopotential model, these used to compute the geoid according to Eqs. (12) and (16), then these results compared with the synthetic geoid heights. The approach that yields the closest fit to the synthetic geoid is assumed to deliver the better data combination.

In addition, the use of a synthetic gravity field avoids the assumptions and approximations introduced by the treatment of the topography and its density variations. This test is considered preferable to the 'conventional' comparison of gravimetric geoid solutions with the discrete geometrical control afforded by ellipsoidal heights and geodetic levelling. This is because the synthetic field has been generated so that it is uncontaminated by errors in these control data.

3.1 Construction of the synthetic field

The EGM96 global geopotential model (Lemoine *et al.*, 1998), complete to $M_{max} = 360$, has been artificially extended into the higher frequencies to construct the synthetic gravity field over

Western Australia. This is similar to the approach of Tziavos (1996), who used a $M_{max} = 360$ geopotential model to generate self-consistent geoid heights and gravity anomalies to test fast Fourier transform (FFT) based techniques. However, the latter only allowed an evaluation in this frequency band and thus prevented a determination of the performance in the higher frequencies and an assessment of the effect of neglecting the truncation error. In order to construct the synthetic gravity field in the higher frequencies, EGM96 has been artificially extended to spherical harmonic degree and order 2700 by artifically creating geopotential coefficients in the region $361 \leq n \leq 2700$ (cf. Holmes *et al.*, 1998). This upper limit was chosen to be commensurate with a spatial resolution of 4' by 4' and is also the point beyond which the fully normalised associated Legendre polynomials start to become numerically unstable.

The fully normalised EGM96 coefficients in the region $361 \leq n \leq 2700$ were generated by recycling the EGM96 coefficients from the orders in degree 360. To ensure that the degree variance of the synthetic gravity field continued to follow a Kaula-type rule in this extended region, a the artifical coefficients ($\overline{C}^*_{nm}$ and $\overline{S}^*_{nm}$) were scaled by $(b/r)^{n-360}$, where b is the semiminor axis length of the reference ellipsoid. From Eq. (3), the synthetic geoid heights are given by

$$N_{syn} = \frac{GM}{r\gamma}\sum_{n=2}^{360}\left(\frac{a}{r}\right)^n\sum_{m=0}^{n}(\delta\overline{C}^{EGM96}_{nm}\cos m\lambda + \overline{S}^{EGM96}_{nm}\sin m\lambda)\overline{P}_{nm}(\cos\theta) + \frac{GM}{r\gamma}\sum_{n=361}^{2700}\left(\frac{a}{r}\right)^n\sum_{m=0}^{n}(\overline{C}^*_{nm}\cos m\lambda + \overline{S}^*_{nm}\sin m\lambda)\overline{P}_{nm}(\cos\theta) \quad . \tag{17}$$

From Eq. (4), the synthetic gravity anomalies are given by

$$\Delta g_{syn} = \frac{GM}{r^2}\sum_{n=2}^{360}\left(\frac{a}{r}\right)^n(n-1)\sum_{m=0}^{n}(\delta\overline{C}^{EGM96}_{nm}\cos m\lambda + \overline{S}^{EGM96}_{nm}\sin m\lambda)\overline{P}_{nm}(\cos\theta) + \frac{GM}{r^2}\sum_{n=361}^{2700}\left(\frac{a}{r}\right)^n(n-1)\sum_{m=0}^{n}(\overline{C}^*_{nm}\cos m\lambda + \overline{S}^*_{nm}\sin m\lambda)\overline{P}_{nm}(\cos\theta) \quad . \tag{18}$$

This synthetic field was relatively easy to implement in the existing computer programs for Eqs. (3) and (4). However, its computation becomes quite time consuming for the high degree components. As such, it is likely that the very high-frequency components of a synthetic gravity field will have to be constructed using alternative means, which are currently under investigation.

3.2 Geoid computation via the 1D-FFT technique

In the mid 1980s, the fast Fourier transform (FFT) technique began to find wide-spread use in gravimetric geoid computation because of its efficient evaluation of convolution integrals when compared to quadrature-based numerical integration. For many years, the planar, two-dimensional FFT was used (eg. Schwarz *et al.*, 1990). Strang van Hees (1990) then introduced the spherical, two-dimensional FFT. However, both of these FFT approaches are subject to approximation errors, the most notable of which is the simplification of Stokes's kernel. Therefore, Forsberg and Sideris (1993) proposed the spherical, multi-band FFT, which reduces the impact of the simplified kernel. Haagmans *et al.* (1993) then refined this approach to give the spherical, one-dimensional FFT, which requires no simplification of Stokes's kernel. For this reason, the 1D-FFT has been used in this investigation so that the exact kernels in Eqs. (11) and (13) can be used without the need for a simplification of the kernel.

Another consideration is that remove-compute-restore determinations of the geoid over a region using the FFT often convolve the whole rectangular grid of gravity anomalies with the spherical Stokes kernel (eg. Sideris and She, 1995). Therefore, this implementation is tested in this study, where in Eq. (12) the spherical integration radius (ψ_0) is replaced by the whole gravity data rectangle. Conversely, quadrature-based geoid determinations using numerical integration of gravity anomalies over a spherical integration radius about each computation point. Therefore, each approach results in a different truncation error due to the neglect of the residual gravity anomalies in the remote zones outside each integration domain.

In order to make the 1D-FFT approach closely mimic quadrature-based numerical integration over a spherical cap, two adaptions of the 1D-FFT approach have been made (Featherstone and Sideris, 1998). The first is the limitation of the integration to a spherical cap by setting the kernel to zero outside the truncation radius (ψ_0) before transformation to the frequency domain. The modified kernel (Eq. 13) was implemented by evaluating it before transformation to the frequency domain. Comparisons with quadrature-based numerical integration software (Featherstone, 1992) were used to verify these adaptions. This approach was used for the computation of AUSGeoid98 (Johnston and Featherstone, 1998), since it allows an efficient evaluation of Eq. (16).

3.3 Comparison of Geoid Results with the Synthetic Model

Equations (17) and (18) were used to construct two, self-consistent 4' by 4' grids of geoid heights and gravity anomalies, respectively, over the region $-11° \leq \phi \leq -37°$ and $112° \leq \lambda \leq 131°$, which covers almost all of the state of Western Australia. These are shown in Figures 1a and 1b and their statistical properties summarised in Table 1. Table 1 also shows the statistical properties of the high-frequency synthetic gravity field, where the $M_{max} = 360$ expansion of EGM96 has been subtracted (cf. Eq. 4).

		max.	min.	mean	st. dev.	rms
total synth. geoid heights	$2 \leq n \leq 2700$	54.979	-40.905	-4.603	22.660	23.123
resid. synth. geoid heights	$361 \leq n \leq 2700$	1.060	-1.061	0.000	0.208	0.208
synth. gravity anomalies	$2 \leq n \leq 2700$	130.459	-188.572	-7.544	34.497	35.312
synth. gravity anomalies	$361 \leq n \leq 2700$	112.531	-122.314	-0.008	21.085	21.085

Table 1. Statistical properties of the synthetic geoid heights (metres) and gravity anomalies (mGal).

The synthetic geoid heights (Eq. 17) were used as control on the tests and the synthetic high-frequency gravity anomalies (Eq. 18; $361 \leq n \leq 2700$) input to the 1D-FFT geoid computation software's implementations of Eqs. (12) and (16). An integration radius of $\psi_0 = 1°$ was used in Eq. (16), since this was the value used in the computation of AUSGeoid98 (Johnston and Featherstone, 1998). No cap radius was specified in Eq. (12) so that the entire gravity data area was used for every geoid computation point. This approach was taken since it replicates the most common FFT-based implementation of the remove-compute-restore technique (eg. Sideris adn She, 1995). The results of the two 1D-FFT geoid computations were compared with the control grid of synthetic geoid heights over the region $-12° \leq \phi \leq -36°$ and $114° \leq \lambda \leq 129°$. This smaller area was chosen so as to eliminate the edge effect associated with the $\psi_0 = 1°$ integration radius. It should be pointed out that this edge effect affects the whole computation area when the cap-radius is unlimited. Nevertheless, the comparisons are conducted over the same area. Table 2 shows a statistical summary of the differences between the control grid of synthetic geoid heights and the results from the 1D-FFT implementations of Eqs. (12) and (16). Figures 1c and 1d show images of these differences, respectively.

		max.	min.	mean	st. dev.	rms
remove-compute-restore	Eq. 12 (ψ_0=1°, $S(\cos\psi)$)	0.058	-0.041	0.008	0.011	0.013
compromise approach	Eq. 16 (ψ_0=π, $S_{20}^{20}(\cos\psi)$)	0.035	-0.035	0.000	0.008	0.008

Table 2. The statistics of the differences between the synthetic control geoid heights and the geoid heights computed from Eqs. (12) and (16) (units in metres).

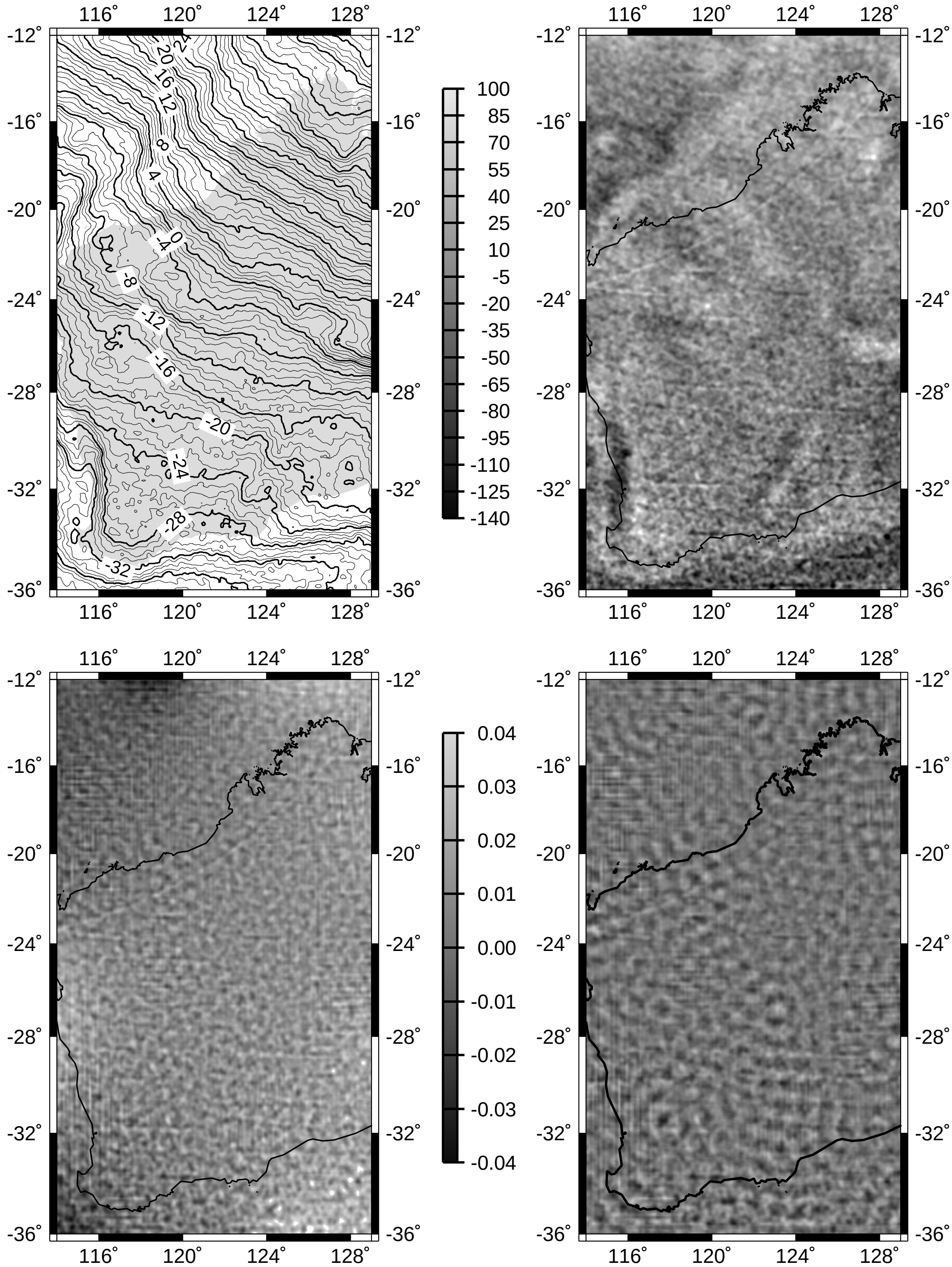

Figure 1. (a) The synthetic geoid heights (m) for $2 \leq n \leq 2700$, (b) The synthetic gravity anomalies (mGal) for $2 \leq n \leq 2700$, (c) The difference (m) between synthetic geoid heights and geoid heights computed from the remove-compute-restore technique (Eq. 12), (d) The difference (m) between synthetic geoid heights and geoid heights computed from the compromise approach (Eq. 16); [Mercator's projection].

4 Discussion, Conclusion and Recommendation

Prior to any discussion, it is essential to point out that the comparisons in Table 2 and between Figures 1c and 1d only consider the effect on the geoid of the neglect of the truncation error and the adaption of the filtering properties by the modified kernel in the high-frequency band ($361 \leq n \leq 2700$). This is because the EGM96 global geopotential model has been used both to construct the synthetic gravity field and produce the residual gravity anomalies in Eq. (4). Accordingly, the filtering and propagation of low-frequency gravity data errors cannot be tested. Future work will introduce low-frequency synthetic data errors in order to study the filtering effects of the kernels in these bands (cf. Vaníček and Featherstone, 1998). Also, using only the high-frequency components has dispensed with the correlations between the data which occur in practice, when using a high-degree, combined global geopotential model.

Nevertheless, the following can be concluded from this band-width-limited study: The improvement offered by the compromised approach in Eq. (16) over the remove-compute-restore approach (Eq. 12) is clearly shown in Table 2. The compromised approach delivers a closer fit to the control grid of geoid heights than does the remove-compute-restore approach. Therefore, the use of the $L = 20$ deterministically modified integration kernel (Eq. 13) over a spherical cap $\psi_0 = 1°$ offers an improvement over the remove-compute-restore technique using the whole computation area. This indicates that the use of a theoretically more appropriate data combination yields better results than simply using more data in the combined solution for the geoid. This is principally because the truncation error has been reduced in size by the kernel modification, thus permitting its neglect, and the filtering properties of the modified kernel lead to a more accurate recovery of the high-frequency geoid undulations. However, due to the considerations described earlier, further work is necessary to quantify their relative effect in other frequency bands so as to replicate the situation in practical geoid computations.

Acknowledgments

I would like to thank the US National Imagery and Mapping Authority, and the US National Aeronautics and Space Administration for providing the EGM96 coefficients and Simon Holmes, a graduate student in the School of Spatial Sciences, for computing the synthetic gravity field.

References

Featherstone WE (1992) A GPS controlled gravimetric determination of the geoid of the British Isles. D.Phil thesis, Oxford University, England.

Featherstone WE, Evans JD, Olliver JG (1998) A Meissl-modified Vaníček and Kleusberg kernel to reduce the truncation error in gravimetric geoid computations. Journal of Geodesy 72(3): 154-160.

Featherstone WE, Sideris MG (1998) Modified kernels in spectral geoid determination: first results from Western Australia, in: Forsberg *et al.* (eds), Geodesy on the Move, Springer, Berlin, 188-193.

Forsberg R, Sideris MG (1993) Geoid computations by the multi-band spherical FFT approach. Bulletin Géodésique 18: 82-90.

Grafarend EW, Engels J (1994) The coinvergent series expansion of the gravitational field of a star-shaped body. manuscripta geodaetica 19: 18-30.

Haagmans RR, de Min E, van Gelderen M (1993) Fast evaluation of convolution integrals on the sphere using 1D-FFT, and a comparison with existing methods for Stokes's integral. manuscripta geodaetica 18(5): 227-241.

Heck B, Grüninger W (1987) Modification of Stokes's integral formula by combining two classical approaches. IUGG General Assembly, Vancouver, Canada.

Heiskanen WH, Moritz H (1967) Physical Geodesy. WH Freeman and Co., San Francisco, USA.

Holmes SA, Featherstone WE, Evans JD (1998) Towards a synthetic Earth gravity model, paper presented to the University of New South Wales Annual Research Seminar, Sydney, November.

Johnston GM, Featherstone WE (1998) AUSGEOID98 computation and validation: exposing the hidden dimension, proceedings of the 39th Australian Surveyors Congress, Launceston, 105-116.

Lemoine FG, Kenyon SC, Factor JK, Trimmer RG, Pavlis NK, Chinn DS, Cox CM, Klosko SM, Luthcke SB, Torrence MH, Wang YM, Williamson RG, Pavlis EC, Rapp RH, Olson TR (1998) The development of the joint NASA GSFC and the National Imagery and Mapping Agency (NIMA) geopotential model EGM96, NASA/TP-1998-206861, National Aeronautics and Space Administration, Maryland, USA.

Martinec Z, Vaníček P (1997) Formulation of the boundary-value problem for geoid determination with a higher-degree reference field. Geophysical Journal International, 126(1): 219-228.

Meissl P (1971) Preparations for the numerical evaluation of second-order Molodensky-type formulas. OSU Report 163, Department of Geodetic Science and Surveying, Ohio State University, Columbus, USA.

Molodensky MS, Eremeev VF, Yurkina MI (1962) Methods for Study of the External Gravitational Field and Figure of the Earth. Israeli Programme for the Translation of Scientific Publications, Jerusalem, Israel.

Paul MK (1973) A method of evaluating the truncation error coefficients for geoidal height, Bulletin Géodésique 47: 413-425.

Schwarz KP, Sideris MG, Forsberg R (1990) The use of FFT techniques in physical geodesy. Geophysical Journal International 100: 485-514.

Sideris MG, She BB (1995) A new, high-resolution geoid for Canada and part of the US by the 1D-FFT method. Bulletin Géodésique 69(2): 92-108.

Sjöberg LE (1991) Refined least squares modification of Stokes's formula. manuscripta geodaetica 16: 367-375.

Stokes GG (1849) On the variation of gravity on the surface of the Earth. Transactions of the Cambridge Philosophical Society 8: 672-695.

Strang van Hees GL (1990) Stokes's formula using fast Fourier techniques. manuscripta geodaetica 15: 235-239.

Torge W (1991) Geodesy (second edition), de Gruyter, Berlin.

Tziavos IN (1996) Comparisons of spectral techniques for geoid computations over large areas. Journal of Geodesy, 70(6): 357-373.

Vaníček P, Kleusberg A (1987) The Canadian geoid — Stokesian approach. manuscripta geodaetica 12(3): 86-98.

Vaníček P, Sjöberg LE (1991) Reformulation of Stokes's theory for higher than second-degree reference field and modification of integration kernels. Journal of Geophysical Research 96(B4): 6529-6539.

Vaníček P, Featherstone WE (1998) Performance of three types of Stokes's kernel in the combined solution for the geoid. Journal of Geodesy 72(11): 684-697.

Vincent S, Marsh JG (1973) Global detailed gravimetric geoid. in: Vies G (ed) Proceedings of the International Symposium on the use of Artificial Earth Satellites for Geodesy and Geodynamics, Athens, Greece, 825-855.

Wenzel H-G (1982) Geoid computation by least-squares spectral combination using integral kernels, Proceedeings of the International Association of Geodesy General Meeting, Tokyo, Japan, 438-453.

Wong L, Gore R (1969) Accuracy of geoid heights from modified Stokes kernels. Geophysical Journal of the Royal Astronomical Society 18: 81-91.